RESEARCH ARTICLE

Aspirin mediates its antitumoral effect through inhibiting PTTG1 in pituitary adenoma

Borbála Szabó[1,2], Kinga Németh[2], Katalin Mészáros[2], Lilla Krokker[1,2], István Likó[2], Éva Saskői[3], Krisztina Németh[4], Pál Tamás Szabó[4], Nikolette Szücs[5], Sándor Czirják[6], Gábor Szalóki[7], Attila Patócs[1,2,3], Henriett Butz[1,2,3].

[1]Department of Laboratory Medicine, Semmelweis University, Budapest, Hungary

[2]Hereditary Tumours Research Group, Hungarian Academy of Sciences - Semmelweis University, Budapest, Hungary

[3]Department of Molecular Genetics and the National Tumor Biology Laboratory, National Institute of Oncology, Budapest, Hungary

[4]MS Metabolomics Research Group, Centre for Structural Study, Research Centre for Natural Sciences, Eötvös Loránd Research Network, Budapest, Hungary.

[5]Department of Endocrinology, Internal Medicine and Oncology, Faculty of Medicine, Semmelweis University, Budapest, Hungary

[6]National Institute of Clinical Neurosciences, Budapest, Hungary.

[7]Department of Pathology and Experimental Cancer Research, Faculty of Medicine, Semmelweis University, Budapest, Hungary

Corresponding author:

Henriett Butz MD, PhD

Hereditary Endocrine Tumours Research Group, Hungarian Academy of Sciences - Semmelweis University, Budapest, Hungary

Department of Laboratory Medicine, Semmelweis University, Budapest, Hungary

Department of Molecular Genetics, National Institute of Oncology, Budapest, Hungary

4. Nagyvárad tér, H-1089, Budapest, Hungary

E-mail: butz.henriett@med.semmelweis-univ.hu

Tel: +36-1-459-1500/56149; +36-20-825-9171

ORCID ID: 0000-0003-1664-409X

Short title: Aspirin inhibits PTTG1 in pituitary adenoma

Keywords: pituitary adenoma, pituitary, PitNET, methylation, demethylation, epigenetic, biomarker, Ptg1

Funding

This work was supported by a Hungarian Scientific Research Grant of the National Research, Development and Innovation Office NKFI FK 135065 to Henriett Butz. HB is a recipient of Bolyai Research Fellowship of the Hungarian Academy of Sciences. H.B and A.P acknowledges financial support from the National Laboratories Excellence program (under the National Tumor Biology Laboratory proiect (NLP17)) and the Hungarian Thematic Excellence Programme (TKP2021-EGA-44).

Authors would like to express their acknowledge to National Program of Bionics (subtheme medical bioinics lead by Attila Patócs). The research was supported by the Higher Education Institutional Excellence Programme of the Ministry of Human Capacities in Hungary, within the framework of the Molecular Biology thematic programme of the Semmelweis University to Attila Patócs.

Disclosure summary

DISCLOSURE STATEMENT: The authors have nothing to disclose

Abstract

Background. DNA demethylation and inhibitory effect of Aspirin on pituitary cell proliferation have been demonstrated.

Our objective was to clarify the molecular mechanisms behind the Aspirin-related effects in pituitary cells.

Materials and Methods. DNA methylome and whole transcriptome profile were investigated in RC4-B/C and GH3 pituitary cell lines upon Aspirin treatment. Effects of Aspirin and demethylation agent, decitabine, were further tested *in vitro*. *PTTG1* expression in 41 human PitNET samples and whole genome gene and protein expression data of 76 PitNET and 34 control samples (available in Gene Expression Omnibus) were evaluated.

Results. Aspirin induced global DNA demethylation and consequential transcriptome changes. Overexpression of *Tet* enzymes and their cofactor *Uhrf2* were identified behind the increase of 5-hydroxymethylcytosine (5hmC). Besides cell cycle, proliferation and migration that were validated by functional experiments, Aspirin increased Tp53 activity through p53 acetylation and decreased E2f1 activity. Among the p53 controlled genes, *Pttg1* and its interacting partners were downregulated upon Aspirin treatment by inhibiting *Pttg1* promoter activity. 5hmC positively correlated with *Tet1-3*, *Tp53* expression, and negatively correlated with *Pttg1* expression that was reinforced by the effect of decitabine. Additionally, high overlap (20.15%) was found between Aspirin regulated genes and dysregulated genes in PitNET tissue samples.

Conclusion. A novel regulatory network has been revealed, where Aspirin regulated global demethylation, *Tp53* activity and *Pttg1* expression along with decreased cell proliferation and migration. 5hmC, a novel tissue biomarker in PitNET, indicated Aspirin antitumoral effect *in vitro* too. Our findings suggest the potential beneficial effect of Aspirin in PitNET.

Introduction

In our previous work we demonstrated the interdependence between DNA demethylation and proliferation behaviour and differentiation stage of pituitary neuroendocrine tumors (PitNET) (1). Indeed, the global DNA demethylation level in tumor tissues negatively correlated with Ki-67 proliferation rate and the ratio of 5-hydroxymetilcitosine (5hmC) to 5-metilcitosine (5mC) was higher in less differentiated adenomas (1). Additionally, increased expression of DNA demethylating enzymes *TET2* and *TET3* was identified as a potential cause behind increased 5hmC level. *TET2-3* exhibited significantly higher expression in adenomas with higher proliferation rate (1). Furthermore, significant positive correlation was detected between TET-cofactor *UHRF2* expression and 5hmC level.

Aspirin (acetylsalicylic acid, ASA), is a commonly used non-steroidal anti-inflammatory drug with antipyretic, analgesic, anti-inflammatory, and anti-thrombotic effect (2). Its antitumoral effect was demonstrated in several cancer types (3), and, epidemiological and clinical studies indicated that Aspirin reduced the cancer risk in several tumor types (3, 4, 5, 6, 7). While these data are encouraging, the mechanisms behind Aspirin antitumoral effect are not entirely clarified. It is partially attributed to the inhibition of cyclooxygenase-2 (COX-2) which is upregulated in various cancer cells (8, 9, 10). Recently, more and more COX-independent effects of Aspirin have been revealed (11, 12). Eventually, ASA regulates multiple signalling pathways, biological functions and molecules including cell cycle, apoptosis, cell differentiation, proteasome and redox-mediated signalling, NF-κB and VEGFs (13, 14, 15). Published data indicated that Aspirin had diverse and complex epigenetic influence too which were implicated in its antitumoral effect (9, 13, 16). Indeed, it was suggested that ASA was able to reverse tumor suppressor gene methylation in cancer tissues. In addition, ASA was shown to modulate histone structure through histone acetylase and deacetylase enzymes (13).

Regarding pituitary, it was also shown that ASA exerted significant inhibitory effect on pituitary adenoma cells directly by targeting cell cycle regulator cyclin A, cyclin dependent kinase 2, and indirectly through decreasing expression of survivin on mRNA and protein levels (17).

Based on these previous findings, in this study our aim was to investigate the genomic and epigenomic effects of ASA in pituitary adenomas using high-throughput profiling approaches (global methylation-demethylation analysis

by HPLC-MS/MS, whole transcriptome sequencing) and validate our findings by targeted methodologies, using *in vitro* functional assays and by investigating human pituitary tissue samples (mRNA microarray).

Methods

Cell culture and treatment. RC-4B/C (CRL-1903) and GH3 (CCL-82.1) pituitary cell lines were obtained from LGC Standards GmbH (Wesel, Germany) in the frame of LGC-ATCC partnership with a corresponding authentication certificate. Cells were cultured as previously we reported (1) following ATCC recommendations, and they were used for experiments between 5-20 passages.

Aspirin (acetylsalicylic acid, ASA) from Sigma Chemical Co. (#A5376, St. Louis, MO, USA) and decitabine from Adooq (#A10292) were purchased and used similarly to our previous published experiments (ASA in 5 mM, decitabine in 10 μM final concentration, as formerly reported) (1, 17).

Patient cohorts. As a discovery cohort, we correlated the methylation/demethylation status of 41 human pituitary adenoma samples that we previously reported (1) with currently measured gene expression data on the same samples (**Table 1**). Tissue samples were collected after surgical removal (National Institute of Clinical Neuroscience, Budapest, Hungary between 2007 and 2017). Histological evaluation performed routinely at the 1st Department of Pathology and Experimental Cancer Research, Semmelweis University, Budapest, Hungary. The histological diagnosis was based on immunohistochemistry for anterior pituitary hormones and transcription factors adequately the 2017 World Health Organization instructions. Altogether, we analyzed 12 GH-producing; 25 gonadotropic (18 FSH/LH +; 7 hormone-negative (HN) SF-1 +); 3 HN, T-pit + corticotropic, and one null cell tissues (1). Patients were informed and consent in writing, and this study was approved by the Scientific and Research Committee of the Medical Research Council of Hungary (0618/15).

For cross-validation, independent cohort of human cases were used: altogether pituitary tissue specimens of 76 non-functioning adenoma and 34 normal samples (**Table 2**). Data of gene and protein expression of these samples were obtained from Gene Expression Omnibus and literature mining (**Table 2**).

Nucleic acid isolation. Total RNA was extracted with Qiagen MiRNeasy Mini kit (217004, Qiagen, Hilden, Germany) or Macherey Nagel NucleoSpin miRNA kit (740971.50, Duren, Germany). Genomic DNA was extracted with QIAamp DNA Mini Kit (51104, Qiagen, Hilden, Germany). The isolation protocol was performed strictly

following the manufacturer's instruction. Nucleic acid purity and quantity were analyzed with NanoDrop 1000 Spectrophotometer (Thermo Fisher Scientific, Waltham, MA, USA.).

DNA methylation-demethylation analysis by high-performance liquid chromatography-tandem mass spectrometry (HPLC-MS/MS).

Chemicals and Reagents. Acetonitrile and formic acid were purchased from VWR International Ltd. (Debrecen, Hungary). Water was prepared by MilliQ Purification System from Millipore (Bedford, MA, USA). 5-methylcytosine and 5-hydroxymethylcytosine DNA Standard Set purchased from Zymo Research Corporation (Biocenter Ltd., Szeged, Hungary).

Sample Preparation. DNA solution containing 1.0 µg DNA was mixed with 50 µL of 98% formic acid and then hydrolyzed at 140 °C for 90 min. The sample was cooled at room temperature and evaporated under nitrogen. The residue was reconstituted in 70 µL acetonitrile-water (50:50, v/v) containing 0.1% formic acid.

LC-MS/MS method were performed as we previously published (18). on an Agilent 1100 Series HPLC coupled with a Sciex 6500 QTRAP tandem mass spectrometer equipped with TurboV ion source instrument.

Transcriptome Sequencing and data analysis. PolyA NGS library preparation was done using NEBNext Ultra II Directional RNA Library Prep Kit for Illumina with Purification Beads (NEB #E7760S/L) strictly following the manufacturer's instruction. Sequencing was run on Illumina Novaseq platform (NovaSeq 6000 SP 300cycles (2x150 bp)) with data output 100M PE reads/sample. Fastq file processing was done using R package. For bioinformatic analysis Bioconductor package edgeR was applied for investigating differential expression. FDR was used for multiple testing correction. Unsupervised cluster analysis was done using Genesis 1.8.1 (https://genome.tugraz.at/genesisclient/genesisclient_news.shtml), t-distributed stochastic neighbour embedding (t-SNE) analysis was performed using iDEP.91 (http://bioinformatics.sdstate.edu/idep/). For pathway analysis gene set enrichment analysis was done using Rno Reactome pathway gene sets. Gene ontology analysis was performed using Generic GO Term Finder. For network construction String database (https://string-db.org/) was applied. For analysing transcription factor regulatory relationships TRRUST was used (https://www.grnpedia.org/trrust/). Raw data will be uploaded to NCBI upon manuscript acceptance.

Gene and protein array expression profile analysis. Briefly, where raw data were available, we reanalysed it using Genespring GX 12 Software (Agilent Tech Inc, Santa Clara, CA, USA) avoiding biases originating from different analysis settings and usage of different softwares. Data analysis details were previously published (19). Fold change filter was set to 2-fold, and then unpaired t-test was used to identify significant ($p< 0.05$) gene expression changes with multiple testing correction (Benjamini-Hochberg). When raw data were not available, significant gene and protein lists extracted from manuscripts and supplementary materials were used (**Table 2**).

In vitro functional assays (viability, proliferation, dead cell ratio, migration, cell cycle analysis and Ki-67 staining by flow cytometry). For determining cell viability Alamar Blue assay (DAL1025, Invitrogen, Thermofisher Scientific, Grand Island, NY, USA) was used on 96 well plates, that is a commonly used method for detection of cell viability and in vitro cytotoxicity. Fluorescent signals with excitation at 560 nm and emission at 590 nm were detected using a flash spectral scanning multimode reader (5250040, Varioskan, Thermofisher Scientific, Waltham, MA, USA) with SkanIt Software 2.4.5 RE. To investigate cell proliferation and dead cell ratio, cell numbers on 6 well plates were determined using 0.4% Trypan Blue staining (15250061, Gibco, Thermofisher Scientific, Waltham, MA, USA).

To assess the effect of ASA on migration wound healing assay was performed on 24 well plate. Following ASA treatment, the cell monolayer was wounded using a 200µL pipette tip and floating cells were washed with PBS (21-040-CV, Corning, Corning, NY, USA.). Photos were taken after 0, 24 and 48 hours and analysed with ImageJ Software (https://imagej.nih.gov/ij/ Bethesda, MD, USA) to calculate cell-free area (CFA %: [(cell-free area 24 or 48h /cell-free area 0h) x 100], and migration rate (cell-covered area (CCA): (100-CFA %) (20).

Cell cycle analysis by flow cytometry. 500 000 cells were incubated with 0.5 ml Cycloscope™ Reagent DNA labeling solution (cat: CYT-CS-R-50; Cytognos, S.L., Salamanca, Spain) for 10 minutes at RT in the dark and then measured with a BD FACS Lyric flow cytometer (Becton, Dickinson and Company, Franklin Lakes, NJ, USA). At least 10 000 events were acquired. Flow cytometry data were analyzed using Kaluza 2.1.1 software (Beckman Coulter, Brea, CA, United States).

Ki-67 staining by flow cytometry. 500 000 cells were fixed for 15 min at RT with 100 µl IntraStain reagent A (Dako-Agilent, CA, USA, cat: K2311). After washing (5 min, 400 x g, RT) with phosphate-buffered saline (PBS, 137 mM NaCl, 2.7 mM KCl, 10 mM Na2HPO4, 1.8 mM KH2PO4, pH = 7.4), the pellet was re-suspended in 100 µl IntraStain

reagent B containing 0.4% Triton X-100 and 5 µl Ki67 antibody (Sony Biotechnology, Weybridge, UK, Cat# 2352515, RRID:AB_2920575). After 15 min incubation at RT in the dark, the cells were washed again (5 min, 400 x g, RT) and the pellet was re-suspended in 0.5 ml PBS containing 0.01 mg/mL 2-(4-Amidinophenyl)-6-indolecarbamidine (DAPI) and incubated for 30 min at RT in the dark. The samples were measured with a BD FACS Lyric flow cytometer (Becton, Dickinson and Company, Franklin Lakes, NJ, USA). At least 50 000 events were acquired. Flow cytometry data were analyzed using Kaluza 2.1.1 software (Beckman Coulter, Brea, CA, United States).

Vector construction and luciferase reporter gene assay were performed as we previously reported (21). Briefly, 2090 bp of the *Pttg1* 5'-UTR 201 ENSRNOT00000005070.5 region was cloned (5′→3′) into pGL3 promoter vector (Promega, Madison, WI) at the 5′ end of the firefly luciferase gene. Activity of *Pttg1*-luc construction was controlled by direct Sanger sequencing and basic luciferase activity detection. RC-4B/C cells were plated at 10^4 cells per well in 96-well plates on the day before transfection. Cells were cotransfected with 150 ng *Pttg1*-luc or control pGL3-promoter plasmid and 150 ng renilla luciferase vector (pRL-TK; Promega, Madison, WI) using Lipofectamine 3000 (Thermofisher Scientific, Grand Island, NY, USA) according to the manufacturer's instructions. Luciferase assay was performed 24 h later using Dual-Glo luciferase assay system (#E2920; Promega, Madison, WI), as previously reported (21).

Targeted gene expression measurements were performed as previously described (1) using TaqMan Gene Expression Assays (ThermoFisher Scientific, Waltham, MA, USA. *Dnmt1*: Rn007009664_m1; *Tet1*: Rn01428192_m1; *Tet2*: Rn01522037_m1; *Tet3*: Rn01425643_m1; *Uhrf1*: Rn02346366_m1; *Uhrf2*: Rn01502134_m1; *Pttg1*: Rn00574373_m1; *Tp53*: Rn00755717_m1 and *PTTG1*: Hs00864094_g1;). Glycerinaldehyde 3-phosphate dehydrogenase (Rn01775763_g1) or β-actin (Hs01060665_g1) were applied as endogenous control. To calculate the relative gene expression changes we used fold change formula [fold change (FC) = 2-ΔΔCt].

Protein extraction and Western Blot were done as we previously reported (17, 22) using the following antibodies: p53 (1C12) mouse mAb (Cell Signaling Technology Cat# 2524, RRID:AB_331743) (1:1000, Cell Signaling Technology, ZA, Leiden, The Netherlands) and acetyl-p53 (K382) rabbit mAB, (1:500, Bioss Cat# bs-0905R, RRID:AB_10855372) (Bioss Antibodies, Woburn, MA, USA); anti-PTTG antibody (DCS-280) (1:2000, Santa Cruz

Biotechnology Cat# sc-56207, RRID:AB_785382) Santa Cruz Biothecnology (Santa Cruz, CA, USA); anti-β-actin (1:1000, Cell Signaling Technology Cat# 4967, RRID:AB_330288) (Cell Signaling Technology, ZA, Leiden, The Netherlands) and secondary antibodies as goat anti-mouse HRP-conjugated (1:2000, Agilent Cat# P0447, RRID:AB_2617137) and goat anti-rabbit HRP-conjugated (1:2000, Agilent Cat# P0448, RRID:AB_2617138) (Agilent, Santa Clara, CA, USA).

Statistical Analysis. Statistical analyses were performed using GraphPad Prism 6.01 software. Results were presented by mean and ± standard deviation (SD). For assessing the differences in DNS methylation/demethylation, cell viability, proliferation and dead cell ratio, mRNA and protein expression unpaired T-test with Welch's correction was used. Investigating correlation between gene expression and methylation/demethylation status Pearson correlation was used. P-values < 0.05 were considered significant.

Data availability. Some or all data generated or analyzed during this study are included in this published article or in the data repositories listed in References.

Results

Methylation-demethylation alteration upon Aspirin treatment

Global methylation-demethylation levels were determined by HPLC-MS/MS following ASA treatment in RC-4B/C and GH3 cells. In RC-4B/C cells significant increase of 5hmC (fold change: 1.95; p=0.0003) and 5hmC/5mC (fold change: 2.49; p=0.0012) ratio were observed (**Figure 1A**). In GH3 cells similar results were detected: both 5hmC (fold change: 3.5; p=0.0005) and 5hmC/5mC ratio were elevated (fold change: 3.28; p=0.0078) (**Figure 1B**). Therefore, expression of enzymes and their cofactors regulating methylation-demethylation circle was measured by RT-qPCR. In line with mass spectrometry result, Dnmt1 responsible for cytosine methylation and its cofactor Uhrf1 showed no change in any of the cell lines (**Figure 1C-D**). However, in RC-4B/C cells, among Tet enzymes (converting 5mC to 5hmC) Tet2, Tet3 and their cofactor Uhrf2 were significantly overexpressed in line with increased 5hmC level (**Figure 1C**). GH3 cells showed very similar expressional alteration, including increased Tet1 level as well (**Figure 1D**). Accordingly, Tet1, 2 and 3 showed significant correlation with 5hmC upon ASA treatment in both cell types (**Figure 1E**).

Global transcriptome alteration upon Aspirin treatment indicates inhibition of cell cycle and proliferation

As global DNA demethylation showed marked alteration after ASA treatment, we investigated its consequence, change in global transcriptome of pituitary cells following 5 mM ASA treatment.

By next generation sequencing 15655 exons belonging to 3278 genes were identified as significant differentially expressed (< or > fold change 2 and FDR $p<0.05$) after 5mM ASA treatment. Unsupervised hierarchical clustering and t-SNE analysis showed that ASA had significant effect on overall gene expression profile (data not shown).

Pathway and gene ontology analysis indicated that the most affected pathway affected was cell cycle (**Table 3**). This was reinforced by network analysis of gene interactions that revealed the top 10 most important genes governing ASA antitumoral effect on transcriptional level (Mad2l1, Pcna, Ube2c, Mcm4, Chek2, Brca1, Smc4, Cdc45, Cdk2, Rbx1) also influenced proliferation, cell division, DNA damage response and ubiquitination.

Several cyclins and cyclin dependent kinase were downregulated, while Cdkn1a was upregulated (**Figure 2A**). The net outcome of ASA effect on cell cycle was represented by the marked decrease of Ki-67 (log2FC: -2.66; p=2.71E-04). In addition, expressional alteration of multiple genes implicated in proliferation, DNA repair and genome stability were identified (**Figure 2B**)

In vitro functional validation of effects of Aspirin on viability, proliferation and cell death

Validation of transcriptional findings using metabolic viability, cell proliferation and cell death of RC-4B/C and GH3 cells by functional *in vitro* assays were carried out. 5 mM ASA led to significant viability decrease of RC-4B/C cells. Inhibition of cell proliferation was also observed as cell number was decreased by 46.5% ($p<0.0001$) (**Figure 3A**). As GH3 cells are characterised by loosely adherent appearance with floating clusters we performed functional assays without media change during ASA treatment. We found slight but significant decrease in viability and cell proliferation by 19.3% (p=0.0028) upon treatment vs. DMSO control. Upon cell cycle analysis by flow cytometry, reduced number of cells entered to the cell cycle and reduced number of cells in S phase were identified in ASA treated group vs. control (4.38% vs. 10.25% and 3.88% vs. 14.94% in RC-4B/C and GH3 cells, respectively.) This

was verified by decreased Ki-67 staining following ASA treatment vs. control: 0.09% vs. 0.34% in RC-4B/C cells and 0.34% vs 1.48% in GH3 cells. ASA resulted in only minor increase 1.66% and 1.11% in dead cell ratio in RC-4B/C and GH3 cells, respectively (**Figure 3A**). Additionally, we observed decreased cellular migration in scratch assay upon ASA treatment (**Figure 3B**).

Aspirin effect on transcription factor activity

Transcription factor regulatory relationships were assessed using RNA sequencing data. Following ASA treatment, genomic effect of 12 transcription factors was revealed (**Table 4**). Among these, Tp53 activity was the most significant. Numerous (25) transcripts regulated by Tp53 showed significant expressional change (**Table 5**). Among *Tp53* controlled genes, *Pttg1* was also identified as downregulated (log2FC: -2.36; p=3,275E-05). E2F1 transcription factor activity was also modulated by ASA, which was also supported by *Birc5* downregulation (log2FC: -1.72; FDR p=0.052). Furthermore, the expression of *Tp53* downstream target Gadd45α was also upregulated (log2FC: 1.90; FDR p=0.0007) upon ASA treatment (**Table 5**).

Although Tp53 expression itself did not change (p=0.475) either in transcriptome data or in validation, ASA led to acetylation at the K382 position and demonstrated significant positive correlation with 5hmC level (**Fig 4A-C**).

Pttg1 is regulated by Aspirin treatment and demethylation in human pituitary adenoma

As Pttg1 is a member in the Tp53 regulatory network and it is a main oncogenic factor in pituitary tumorigenesis, we investigated the expression of Pttg1 further. We found that genes regulated by Pttg1and Pttg1 interacting partners were downregulated (**Figure 5A**) after ASA treatment. Besides Pttg1 interaction partners, Pttg1 expression was significantly decreased on mRNA and protein level as well (Pttg1 protein level decreased to 49%±2% in RC-4B/C and to 31%±22% in GH3 cells, respectively) (**Figure 5A**).

By constructing a *Pttg1* promoter reporter system, we observed marked decrease in *Pttg1* promoter activity upon ASA treatment. Additionally, as upon ASA administration significant negative correlation was observed between *Pttg1* expression and 5hmC level (**Figure 5B**) we also investigated the effect of global demethylation agent,

decitabine on *Pttg1* promoter. We found that decitabine decreased *Pttg1* promoter activity *in vitro*. However, in human pituitary adenomas global methylation and demethylation level did not show significant association with PTTG1 expression (**Figure 5C**)

Aspirin regulated gene signature can be detected in human pituitary adenoma samples

To cross-validate ASA effect, transcriptome and protein expression of independent human pituitary adenoma samples (76 adenoma and 34 normal control specimen) were used (**Table 2**). Using the differentially expressed genes between human adenomas and normal specimens (3755 genes), we filtered out those which were also regulated by ASA. High proportion, 20.15% of the genes (757/3755) dysregulated in human PitNET samples were common with ASA regulated genes. The 757 common genes were implicated mostly in cell proliferation, cell cycle – including p53 activity and function, while cellular migration and genome stability were also detected (**Table 6**).

Discussion

Based on our previous findings that in PitNET DNA demethylation was altered and it showed correlation with proliferative behavior and differentiation (1) and the Aspirin epigenetic effects in other malignancies (13) we investigated the complex genomic and epigenomic consequences of Aspirin treatment in PitNET.

Upon Aspirin treatment increased global DNA demethylation was observed. In line with this, the overexpression of Tet1, 2 and 3 (enzymes responsible for DNA demethylation) and their cofactor Uhrf2 were confirmed. In addition, DNA methylation machinery did not show significant change (either the global level of 5mC or Dnmt1 or its cofactor Uhrf1 did not exhibit alteration). As accurate measurements and detection of demethylation (5hmC) is challenging and requires special instrumentation, only scarce information have been available regarding demethylation change upon Aspirin treatment. In a study using methylation specific PCR, Guo et al demonstrated that Aspirin induced demethylation of the Forkhead Box D3 (*FOXD3*) promoter leading to increased FOXD3 expression (23). They also proved that regular use of Aspirin dramatically decreased the number of metastatic nodules of cancer cells in immunodeficient mouse lungs through FOXD3-OLA1P2-STAT3 axis (23). Similarly, we demonstrated that *Pttg1* promoter activity and expression were decreased by Aspirin and by the demethylation agent,

decitabine treatment, respectively (**Figure 6**). In addition, a negative correlation was observed between Pttg1 expression and 5hmC level indicating the link between Aspirin, demethylation and Pttg1 expression change.

As a consequence of global demethylation significant transcriptome alteration was observed using whole RNA sequencing. Investigating the biological function of altered transcriptome profile, mainly cell cycle and proliferation related transcriptional changes were observed. Changes in viability, proliferation and cellular migration of pituitary cells were also validated by multiple *in vitro* functional assays. All these are in line with our previous finding, that the global increase of demethylation correlated with Ki-67 proliferation index measured in human PitNET tissue samples (1). In addition, cell division and pituitary cell migration were also found to be inhibited by Aspirin. However, the exact mechanism has to be further investigated it could be hypothesized that this occurred through Pttg1 regulated Aurka and Aurkb downregulation (see details below), because Aurka regulates cilia disassembly, neurite extension, cell motility, while Aurkb was also described to reduce cellular migration of tumor cells (24, 25).

Analyzing transcription factor regulatory relationships, Tp53 and E2f1 showed most significant alteration in activity. Indeed, the transcription factor E2f1, is a key cell cycle regulator and it targets genes encoding proteins that regulate cell cycle progression through the G1/S transition (26). Therefore, its reduced activity upon Aspirin treatment was further confirmed by our *in vitro* functional results. While the expression of Tp53 did not change significantly upon Aspirin administration, the change in its activity was experienced by the transcriptional outcome as genes regulated by Tp53 showed significant enrichment upon Aspirin treatment. In the background we detected increased Tp53 acetylation at the lysine residue at 382 position, that was previously shown to stabilize Tp53 protein and increase its transcriptional activity (27) (**Figure 6**). Furthermore, Tp53 expression showed positive correlation with 5hmC level. As 5hmC is an indicator of decreased proliferation, our findings recapitulated previous data that Aspirin acetylated and thereby activated Tp53 and induced Cdkn1a (p21) in colon tumors (28). Additionally, in PitNET cells ASA also led to elevated Cdkn1a expression reflecting the increased Tp53 activity.

As Pttg1 is a well-known oncogene in pituitary tumorigenesis, it is overexpressed in approximately 90% of pituitary adenomas (29), and it is a member of Tp53 interaction partners, we further investigated its expression and activity upon Aspirin treatment. Aspirin effectively decreased Pttg1 expression in pituitary adenoma both on RNA and protein level demonstrated by NGS, qPCR and western blot analysis. Additionally, members of the Pttg1

regulatory network also showed decreased expression indicating decreased *Pttg1* activity. Also, upon Aspirin treatment of pituitary adenoma cells, a significant negative correlation was observed between Pttg1 and 5hmC indicating the link between the two. Moreover, high proportion (20.15%) of genes being common between Aspirin regulated genes and dysregulated genes in human pituitary adenomas further indicates that Aspirin may have a beneficial effect in this tumor type. These results are in line with previously ones, demonstrating that PTTG1 interacted with p53 and in cooperation with PTTG1 binding factor (PBF) it reduced p53 protein stability (30). Altogether, p53 and PTTG1 showed negative correlation, and head and neck squamous cell carcinoma patients with high tumoral PTTG1 had the poorest overall survival, which reflected a marked impairment of p53-dependent signaling (30).

As a summary, Aspirin has antitumoral effects in multiple levels in pituitary adenoma, summarized on **Figure 6**. However, additional links can also be revealed from transcription alterations. For instance, the Tp53 downstream target Gadd45α, that is upregulated upon ASA treatment, besides inhibiting proliferation through its interaction with *Pcna* and regulating DNA repair, it also induces global DNA hypomethylation (31). Aurkb, the mitosis regulator, is induced by *Pttg1* and *E2f1*. As our findings on rat pituitary tumor cells (negative correlation of 5-hmC with Ki-67) were in line with previous results described in human PitNET specimens (1), therefore, we can hypothesize, that the modulation of 5-hmC by ASA or decitabine and associated inhibition of Pttg1 may have antiproliferative effect on human PitNET as well. Nevertheless, our results should be validated in human PitNET samples as well, in order to avoid potential inter-species differences.

Conclusion

Aspirin exerted its antitumoral effects among others, on genomic and epigenomic levels in pituitary cells. An Aspirin-demethylation-*Pttg1* regulatory network was described as an antitumoral mechanism in pituitary. 5hmC, a previously identified biomarker correlating with Ki-67 and differentiation of PitNET, also indicated the antitumoral effect of Aspirin. Additionally, in the high overlap between the human pituitary transcriptome changes and Aspirin regulated gene signature further suggest the potential beneficial effect of Aspirin in PiTNET, however further studies are necessary to strengthen this finding.

References

1. Szabó B, Németh K, Mészáros K, Szücs N, Czirják S, Reiniger L, Rajnai H, Krencz I, Karászi K, Krokker L, Patócs A, & Butz H. Demethylation Status of Somatic DNA Extracted From Pituitary Neuroendocrine Tumors Indicates Proliferative Behavior. *The Journal of Clinical Endocrinology & Metabolism* 2020 **105** 2015–2026. (doi:10.1210/clinem/dgaa156)

2. Patrono C & Rocca B. Aspirin and Other COX-1 inhibitors. *Handbook of Experimental Pharmacology* 2012 137–164. (doi:10.1007/978-3-642-29423-5_6)

3. Ma J, Cai Z, Wei H, Liu X, Zhao Q, & Zhang T. The anti-tumor effect of aspirin: What we know and what we expect. *Biomedicine & Pharmacotherapy* 2017 **95** 656–661. (doi:10.1016/j.biopha.2017.08.085)

4. Hua H, Zhang H, Kong Q, Wang J, & Jiang Y. Complex roles of the old drug aspirin in cancer chemoprevention and therapy. *Medicinal Research Reviews* 2019 **39** 114–145. (doi:10.1002/med.21514)

5. Bosetti C, Gallus S, & La Vecchia C. Aspirin and cancer risk: an updated quantitative review to 2005. *Cancer causes & control: CCC* 2006 **17** 871–888. (doi:10.1007/s10552-006-0033-7)

6. Cuzick J, Otto F, Baron JA, Brown PH, Burn J, Greenwald P, Jankowski J, La Vecchia C, Meyskens F, Senn HJ, & Thun M. Aspirin and non-steroidal anti-inflammatory drugs for cancer prevention: an international consensus statement. *The Lancet. Oncology* 2009 **10** 501–507. (doi:10.1016/S1470-2045(09)70035-X)

7. Dovizio M, Tacconelli S, Sostres C, Ricciotti E, & Patrignani P. Mechanistic and Pharmacological Issues of Aspirin as an Anticancer Agent. *Pharmaceuticals* 2012 **5** 1346–1371. (doi:10.3390/ph5121346)

8. Khan MNA & Lee YS. Cyclooxygenase inhibitors: scope of their use and development in cancer chemotherapy. *Medicinal Research Reviews* 2011 **31** 161–201. (doi:10.1002/med.20182)

9. Zhang X, Du R, Luo N, Xiang R, & Shen W. Aspirin mediates histone methylation that inhibits inflammation-related stemness gene expression to diminish cancer stemness via COX-independent manner. *Stem Cell Research & Therapy* 2020 **11** 370. (doi:10.1186/s13287-020-01884-4)

10. Qadri SSA, Wang JH, Redmond KC, O'Donnell AF, Aherne T, & Redmond HP. The role of COX-2 inhibitors in lung cancer. *The Annals of Thoracic Surgery* 2002 **74** 1648–1652. (doi:10.1016/S0003-4975(02)04022-5)

11. Alfonso L, Ai G, Spitale RC, & Bhat GJ. Molecular targets of aspirin and cancer prevention. *British Journal of Cancer* 2014 **111** 61–67. (doi:10.1038/bjc.2014.271)

12. Chen Z, Li W, Qiu F, Huang Q, Jiang Z, Ye J, Cheng P, Low C, Guo Y, Yi X, Chen W, Yu Y, Han Y, Wu J, Jin S, Kong D, & Huang J. Aspirin cooperates with p300 to activate the acetylation of H3K9 and promote FasL-mediated apoptosis of cancer stem-like cells in colorectal cancer. *Theranostics* 2018 **8** 4447–4461. (doi:10.7150/thno.24284)

13. Yiannakopoulou E. Targeting epigenetic mechanisms and microRNAs by aspirin and other non steroidal anti-inflammatory agents - implications for cancer treatment and chemoprevention. *Cellular Oncology* 2014 **37** 167–178. (doi:10.1007/s13402-014-0175-7)

14. Yiannakopoulou E. Modulation of lymphangiogenesis: a new target for aspirin and other nonsteroidal anti-inflammatory agents? A systematic review. *Journal of Clinical Pharmacology* 2012 **52** 1749–1754. (doi:10.1177/0091270011431066)

15. Dovizio M, Bruno A, Tacconelli S, & Patrignani P. Mode of action of aspirin as a chemopreventive agent. *Recent Results in Cancer Research. Fortschritte Der Krebsforschung. Progres Dans Les Recherches Sur Le Cancer* 2013 **191** 39–65. (doi:10.1007/978-3-642-30331-9_3)

16. Guo Y, Liu Y, Zhang C, Su ZY, Li W, Huang MT, & Kong AN. The epigenetic effects of aspirin: the modification of histone H3 lysine 27 acetylation in the prevention of colon carcinogenesis in azoxymethane- and dextran sulfate sodium-treated CF-1 mice. *Carcinogenesis* 2016 **37** 616–624. (doi:10.1093/carcin/bgw042)

17. Németh K, Szücs N, Czirják S, Reiniger L, Szabó B, Barna G, Karászi K, Igaz P, Zivkovic V, Korbonits M, Patócs A, & Butz H. Survivin as a potential therapeutic target of acetylsalicylic acid in pituitary adenomas. *Oncotarget* 2018 **9** 29180–29192. (doi:10.18632/oncotarget.25650)

18. Németh K, Mészáros K, Szabó B, Butz H, Arányi T, & Szabó PT. A relative quantitation method for measuring DNA methylation and hydroxymethylation using guanine as an internal standard. *Analytical Methods: Advancing Methods and Applications* 2021 **13** 4614–4622. (doi:10.1039/d1ay00897h)

19. Butz H, Szabó PM, Nofech-Mozes R, Rotondo F, Kovacs K, Mirham L, Girgis H, Boles D, Patocs A, & Yousef GM. Integrative Bioinformatics Analysis Reveals New Prognostic Biomarkers of Clear Cell Renal Cell Carcinoma. *Clinical Chemistry* 2014 **60** 1314–1326. (doi:10.1373/clinchem.2014.225854)

20. Butz H, Szabó PM, Khella HWZ, Nofech-Mozes R, Patocs A, & Yousef GM. miRNA-target network reveals miR-124as a key miRNA contributing to clear cell renal cell carcinoma aggressive behaviour by targeting CAV1 and FLOT1. *Oncotarget* 2015 **6** 12543–12557. (doi:10.18632/oncotarget.3815)

21. Butz H, Likó I, Czirják S, Igaz P, Khan MM, Zivkovic V, Bálint K, Korbonits M, Rácz K, & Patócs A. Down-Regulation of Wee1 Kinase by a Specific Subset of microRNA in Human Sporadic Pituitary Adenomas. *The Journal of Clinical Endocrinology & Metabolism* 2010 **95** E181–E191. (doi:10.1210/jc.2010-0581)

22. Butz H, Németh K, Czenke D, Likó I, Czirják S, Zivkovic V, Baghy K, Korbonits M, Kovalszky I, Igaz P, Rácz K, & Patócs A. Systematic Investigation of Expression of G2/M Transition Genes Reveals CDC25 Alteration in Nonfunctioning Pituitary Adenomas. *Pathology oncology research: POR* 2017 **23** 633–641. (doi:10.1007/s12253-016-0163-5)

23. Guo H, Liu J, Ben Q, Qu Y, Li M, Wang Y, Chen W, & Zhang J. The aspirin-induced long non-coding RNA OLA1P2 blocks phosphorylated STAT3 homodimer formation. *Genome Biology* 2016 **17** 24. (doi:10.1186/s13059-016-0892-5)

24. Bertolin G & Tramier M. Insights into the non-mitotic functions of Aurora kinase A: more than just cell division. *Cellular and molecular life sciences: CMLS* 2020 **77** 1031–1047. (doi:10.1007/s00018-019-03310-2)

25. Porcelli L, Guida G, Quatrale AE, Cocco T, Sidella L, Maida I, Iacobazzi RM, Ferretta A, Stolfa DA, Strippoli S, Guida S, Tommasi S, Guida M, & Azzariti A. Aurora kinase B inhibition reduces the proliferation of metastatic melanoma cells and enhances the response to chemotherapy. *Journal of Translational Medicine* 2015 **13** 26. (doi:10.1186/s12967-015-0385-4)

26. Sheldon LA. Inhibition of E2F1 activity and cell cycle progression by arsenic via retinoblastoma protein. *Cell Cycle (Georgetown, Tex.)* 2017 **16** 2058–2072. (doi:10.1080/15384101.2017.1338221)

27. Reed SM & Quelle DE. p53 Acetylation: Regulation and Consequences. *Cancers* 2014 **7** 30–69. (doi:10.3390/cancers7010030)

28. Ai G, Dachineni R, Kumar DR, Marimuthu S, Alfonso LF, & Bhat GJ. Aspirin acetylates wild type and mutant p53 in colon cancer cells: identification of aspirin acetylated sites on recombinant p53. *Tumour Biology: The Journal of the International Society for Oncodevelopmental Biology and Medicine* 2016 **37** 6007–6016. (doi:10.1007/s13277-015-4438-3)

29. Tfelt-Hansen J, Kanuparthi D, & Chattopadhyay N. The Emerging Role of Pituitary Tumor Transforming Gene in Tumorigenesis. *Clinical Medicine and Research* 2006 **4** 130–137.

30. Read ML, Modasia B, Fletcher A, Thompson RJ, Brookes K, Rae PC, Nieto HR, Poole VL, Roberts S, Campbell MJ, Boelaert K, Turnell AS, Smith VE, Mehanna H, & McCabe CJ. PTTG and PBF Functionally Interact with p53 and Predict Overall Survival in Head and Neck Cancer. *Cancer Research* 2018 **78** 5863–5876. (doi:10.1158/0008-5472.CAN-18-0855)

31. Tamura RE, Vasconcellos JF de, Sarkar D, Libermann TA, Fisher PB, & Zerbini LF. GADD45 proteins: central players in tumorigenesis. *Current Molecular Medicine* 2012 **12** 634–651. (doi:10.2174/156652412800619978)

Figures and Tables

Table 1. Discovery sample cohort

Sex	Age	Clinical diagnosis	cell lineage	Immunhistochemistry	Ki 67 (%)	Ellipsoid volume (mm^3)	primary/ recurrent
F	76	NFPA	gonadotroph	FSH	2-3%	1767	primary
M	44	NFPA	gonadotroph	FSH	2-3%	n.a.	primary
M	51	NFPA	gonadotroph	FSH	2-3%	10	recurrent
F	39	NFPA	gonadotroph	FSH	1-2%	n.a.	primary
M	38	NFPA	gonadotroph	FSH	3-4%	n.a.	primary
F	49	NFPA	gonadotroph	FSH, LH	<1%	1950	recurrent
F	74	NFPA	gonadotroph	FSH, LH	< 3%	n.a.	primary
M	62	NFPA	gonadotroph	FSH, LH	<3%	n.a.	primary
M	64	NFPA	gonadotroph	FSH, LH	< 3%	87114	primary
M	63	NFPA	gonadotroph	FSH, LH	<1%	21501	primary
F	68	NFPA	gonadotroph	FSH, LH	3-4%	n.a.	recurrent
M	43	NFPA	gonadotroph	FSH, LH	7-10%	n.a.	primary
F	37	NFPA	gonadotroph	FSH,LH	7-8%	1150	recurrent
F	80	NFPA	gonadotroph	FSH,LH	2-3%	16366	primary
M	73	NFPA	gonadotroph	FSH,LH	2-3%	n.a.	primary
M	38	NFPA	gonadotroph	FSH,LH	3-4%	n.a.	primary
M	73	NFPA	gonadotroph	LH	2%	5964	primary
M	72	NFPA	gonadotroph	LH	< 2%	2145	primary
M	50	NFPA	gonadotroph	T-Pit -; PIT1 - ; SF-1 +	<2%	n.a.	recurrent
F	64	NFPA	gonadotroph	T-Pit -; PIT1 - ; SF-1 +	5%	n.a.	primary
F	60	NFPA	gonadotroph	T-Pit -; PIT1 - ; SF-1 +	5%	n.a.	recurrent
M	58	NFPA	gonadotroph	T-Pit -; PIT1 - ; SF-1 +	5-7%	14137	primary
F	64	NFPA	gonadotroph	T-Pit -; PIT1 -; SF-1 +	< 1%	n.a.	primary
F	50	NFPA	gonadotroph	T-Pit -; PIT1 -; SF-1 +	2%	n.a.	primary
F	43	NFPA	gonadotroph	T-Pit -; PIT1 -; SF-1 +	1%	n.a.	primary
F	58	NFPA	corticotroph	T-Pit + ; PIT1 - ; SF-1 -	4%	1950	primary
F	65	NFPA	corticotroph	T-Pit + ; PIT1 - ; SF-1 -	3-4%	905	primary
F	49	NFPA	corticotroph	T-Pit + ; PIT1 - ; SF-1 -	3-4%	n.a.	primary
M	73	NFPA	null cell	T-Pit -; PIT1 - ; SF-1 -	3-4%	6371	recurrent
M	35	GH-producing	somatotoph,lactototroph	GH, PRL	6%	n.a.	primary
M	30	GH-producing	somatotoph,lactototroph	GH, PRL	8%	2185	primary
M	51	GH-producing	somatotoph,lactototroph	GH, PRL	< 3%	n.a.	primary
F	22	GH-producing	somatotoph,lactototroph	GH, PRL	4-5%	n.a.	recurrent
F	35	GH-producing	somatotoph,lactototroph	GH, PRL	5-6%	n.a.	recurrent
F	48	GH-producing	somatotoph,lactototroph	GH, PRL	10%	n.a.	primary

M	22	GH-producing	somatotoph,lactototroph	GH, PRL	3%	8181	primary
F	49	GH-producing	somatotoph,lactototroph	GH, PRL	3-4%	1023	primary
M	33	GH-producing	somatotoph,lactototroph	GH, PRL	3-4%	n.a.	primary
F	60	GH-producing	somatotoph,lactototroph	GH, PRL	< 3%	n.a.	primary
M	49	GH-producing	somatotoph	GH	< 1%	n.a.	recurrent
F	43	GH-producing	somatotoph	GH	1-3%	n.a.	primary

Table 2. Validation sample cohort

	# of pituitary adenoma samples (NFPA)	# of normal control samples (NP)	Platform (used data)
Gene expression studies			
Morris et al. 2005	5	5	Affymetrix HG-U133 Plus 2.0 Array (GEO Acc. Number: GSE2175)
Michaelis et al. 2011	14	9	Affymetrix HG-U133A Array (GEO Acc. Number: GSE26966)
Moreno et al. 2005	11	3	Affymetrix HG-U95A V.2 Array (significant gene list published)
Elston et al. 2008	13	3	Affymetrix HG-U133 Plus 2.0 Array (significant gene list published)
Feng et al. 2015	7	3	Agilent-014850 Whole Human Genome Microarray (GEO Acc. Number: GSE51618)
Protein array studies			
Moreno et al. 2005	11	3	2DGE-MS (significant protein list published)
Zhan et al. 2010	15	8	2DGE-MS (significant protein list published)

Table 3. Pathway analysis of transcriptional changes upon ASA treatment (only the first 10 significant pathways are presented)

Reactome patway ID	**Reactome patway Name**	**observed gene count**	**background gene count**	**false discovery rate**
RNO-69278	Cell Cycle, Mitotic	71	387	4.82e-06
RNO-1640170	Cell Cycle	77	449	7.19e-06
RNO-1430728	Metabolism	162	1330	0.00035
RNO-194315	Signaling by Rho GTPases	56	324	0.00035
RNO-69306	DNA Replication	27	102	0.00035
RNO-194840	Rho GTPase cycle	28	117	0.00058
RNO-453279	Mitotic G1-G1/S phases	26	103	0.00058
RNO-69002	DNA Replication Pre-Initiation	20	65	0.00058
RNO-69620	Cell Cycle Checkpoints	41	218	0.00058
RNO-68886	M Phase	48	283	0.00097

Table 4. Activity of transcription factors changed following aspirin treatment

Transcription factor	P-value	Adjusted P-value	Genes regulated by the transcription factor
TP53	9.244E-9	5.28E-06	*MCM7; MKI67; FOXM1; AQP3; EGFR; RECQL4; CCNB1; PTTG1; GPNMB; CHEK2; CASP3; E2F7; PDGFRB; PLK3; SMAD3; GADD45A; GDF15; PLK1; CCNA2; PRC1; CDK1; CRYAB; ATF3; MAD1L1; EZH2*
E2F1	8.646E-8	2.47E-05	*TOP2A; RRM1; RRM2; HSPA5; PLK1; FANCA; CDC6; FOXM1; AURKB; AURKA; DHFR; CCNB1; RAD51; CHEK2; DDIT3; CDK1; MYBL2; KIF2C; MCM5; ECT2; ASF1B*
E2F4	1.851E-6	3.52E-04	*PLK4; CCNB1; RAD51; PLK1; PCLAF; MCM10; TTK; AURKB*
E2F3	5.498E-6	7.85E-04	*CCNA2; CCNB1; PLK1; CDK1; CDC6; AURKA*
TRP53	1.265E-5	0.001445	*PDGFRB; DUSP4; PLK3; SMAD3; MCM7; GADD45A; GDF15; INSR; FOXM1; CKS1B; CCNA2; PER2; CCNB1; GAP43; KRT19; COL2A1; CASP3; PCBP2; PTGDS; ATF3*
E2F4	2.181E-5	0.002076	*PLK4; MAP1LC3B; RAD51; E2F2; MYBL2*
TFAP2A	1.144E-4	0.009333	*ACHE; CCNB1; CRABP2; GALNT3; TH; CYP11A1; MCAM; CGA; ADRA1A; CRYAB; EGFR*
ATF1	2.953E-4	0.021081	*TOP2A; LDHA; MAP1LC3B; TH; SLC20A1; CGA*
ATF4	4.086E-4	0.025929	*MAP1LC3B; HSPA5; DDIT3; TRIB3; NDC80; ATF3; DDR2*
TFDP1	4.440E-4	0.025353	*DHFR; RRM1; CDK1; MYBL2*
XBP1	7.446E-4	0.038652	*ERN1; HSPA5; GAD1; DDIT3; ERP29*
ARNT	9.602E-4	0.045694	*JUN; GAD1; BHLHE40; AHR; MFSD2A*

Table 5. Expression changes of genes from Tp53 regulatory network

GeneName	EnsGeneID	log2FC	p Value	FDR
Aqp3	ENSRNOG00000009797	-2.30422	5E-05	0.001157
Atf3	ENSRNOG00000003745	3.484486	1.43E-08	1.8E-06
Casp3	ENSRNOG00000010475	-2.04182	1.61E-06	6.51E-05
Ccna2	ENSRNOG00000015423	-2.64293	0.02121	0.050602
Ccnb1	ENSRNOG00000058539	-2.99567	9.47E-09	1.09E-06
Cdk1	ENSRNOG00000000632	-2.13709	1.25E-05	0.000341
Chek2	ENSRNOG00000037509	-1.37363	0.0324	0.083205

Cryab	ENSRNOG00000010524	2.61213	0.000107	0.002052
E2f7	ENSRNOG00000026252	-3.02489	0.000156	0.002484
Egfr	ENSRNOG00000004332	1.951245	0.000199	0.003023
Ezh2	ENSRNOG00000006048	-1.18708	0.01809	0.067119
Foxm1	ENSRNOG00000005936	-2.53223	1.17E-06	5.55E-05
Gadd45a	ENSRNOG00000005615	1.907358	3.82E-05	0.000778
Gdf15	ENSRNOG00000019661	2.696207	2.61E-06	0.000124
Gpnmb	ENSRNOG00000008816	2.678566	3.31E-08	2.54E-06
Mad1l1	ENSRNOG00000001265	-1.90029	0.000841	0.009182
Mcm7	ENSRNOG00000001349	-2.1472	2.97E-05	0.000535
Mki67	ENSRNOG00000028137	-2.66258	1.47E-05	0.000271
Pdgfrb	ENSRNOG00000018461	2.073018	0.002211	0.014145
Plk1	ENSRNOG00000018815	-2.84073	7.04E-09	8.9E-07
Plk3	ENSRNOG00000018484	1.98987	8.11E-06	0.000296
Pprc1	ENSRNOG00000018561	-0.15577	0.587733	0.749968
Pttg1	ENSRNOG00000003802	-2.35927	5.87E-07	3.28E-05
Recql4	ENSRNOG00000032446	-1.78421	0.000247	0.00399
Smad3	ENSRNOG00000008620	1.545729	0.001247	0.009008
Tp53	ENSRNOG00000010756	-0.40314	0.300957	0.475431

Table 6. Pathway analysis of commonly regulated genes between human pituitary adenoma vs. normal pituitary and Aspirin regulated genes. *B&H: Benjamini-Hochberg false discovery rate adjustment*.

Category	Name	Source*	q-value FDR B&H	# of affected gene nr / # of genes of pathway	ratio of affected genes in the pathway
p53-related pathways	p53 Signaling Pathway	1	3.507E-2	5/16	0.3125
	Direct p53 effectors	2	4.360E-2	15/132	0.113636
Proliferation and cell division related pathways	Retinoblastoma Gene in Cancer	1	6.484E-6	20/88	0.227273
	DNA strand elongation	4	9.949E-5	11/32	0.34375
	DNA replication	3; 1	1.188E-3	10/36	0.277778
	Regulation of nuclear SMAD2/3 signaling	2; 1	2.005E-2	12/77	0.155844
	G1 to S cell cycle control	1	3.507E-2	10/64	0.15625
Genome stability related pathways	Activation of ATR in response to replication stress	4	2.193E-2	8/37	0.216216

Sources*: 1: MSigDB C2 BIOCARTA (v7.3); 2: BioSystems: Pathway Interaction Database; 3: BioSystems: KEGG; 4: BioSystems: REACTOME.

Figure Legends

Figure 1. ASA effect on DNA methylation-demethylation. Change of global methylation-demethylation in RC-4B/C (A) and in GH3 (B) cells. (C) Gene expression change behind global methylation/demethylation in RC-4B/C (C) and in GH3 (D) cells. (E) Correlation between 5hmC and demethylation enzymes

Figure 2. (A) Gene expression change behind cell cycle and proliferation alteration upon aspirin administration. Expression of genes implicated in cell cycle phase G1, S, G2 and M are indicated by blue, green, yellow and red, respectively. Expressions of genes that inhibit cell cycle are illustrated by grey color. (B) ASA genomic effect in

pituitary adenoma. Expression changes: *Tp53* (log2CPM:-0.403135161, FDR:0.475431307); *E2f1* (log2CPM:-1.699322161, FDR:0.017677985); *Birc5* (log2CPM:-1.669861341, FDR:0.002634309); *Aurka* (log2CPM:-2.693827176, FDR:0.000112511); *Aurkb* (log2CPM:-1.994711397, FDR:0.009565016); *Pttg1* (log2CPM:-2.359268022, FDR:3.27562E-05); *Ha2x* (log2CPM:-1.59, FDR:5.86E-03); *Ezh2* (log2CPM:-1.187080264, FDR:0.067119053); *Ccnb1* (log2CPM:-2.995668611, FDR:1.09241E-06); *Ccne1* (log2CPM:-1.533242072, FDR:0.015933026); *Ccna2* (log2CPM:-2.642928343, FDR:0.050601632); *Cdk1* (log2CPM:-2.137090443, FDR:0.000341413); *Cdkn1a* (log2CPM:1.591983374, FDR:0.003852956); *Gadd45a* (log2CPM:1.907358455, FDR:0.000777632). Genes indicated by grey represent links between the transcriptional and epigenomic level. See further details in the discussion.

Figure 3. *In vitro* validation. (A) microscopic images of RC-4B/C and GH3 cells upon ASA treatment for morphological assessment: significant morphologic changes cannot be observed upon DMSO or ASA treatment, only reduced cell numbers are suggested in ASA group. (B) Decreased optical density following ASA treatment was observed compared to controls, due to decreased proliferation. No cytotoxic effect of DMSO was observed vs. non-treated (NT) group. (C) ASA effect on cell proliferation was further investigated by living cell numbers. Cell proliferation was 46% ($p<0.0001$) and 80% ($p=0.028$) in ASA group vs. DMSO control in RC-4B/C and GH3 cells, respectively. Significant cell death was not observed in either cell lines upon treatment. (D) Cell cycle analysis by flow cytometry indicated reduced number of cells entering to the cell cycle and reduced number of cells in S phase upon ASA treatment vs. control (4.38% vs. 10.25% and 3.88% vs. 14.94% in RC-4B/C and GH3 cells, respectively). (E) ASA decreased RC-4B/C cell migration to 34% ($p=0.01$) and 47% ($p=0.02$) for 24 and 48h, respectively.

Figure 4. (A) *Tp53* expression in transcriptome and RT-qPCR validation. (B) *Tp53* significantly correlated with 5hmC upon ASA administration. (C) Western blot indicated no total p53 protein change following ASA treatment, however, treatment induced p53 acetylation at K382 residue. Densitometry showing the ratio acetyl-p53/total p53. Due to the lack of total p53 band in RC-4B/C cell, and the lack of acetylated p53 in the untreated cells, the ratio acetyl-p53/total p53 can be given only for MDA-MB231 and GH3 cells and it should be interpreted with caution

Figure 5. (A) Transcriptional change of *Pttg1* and its interaction partners upon ASA effect. Decreased levels of *Pttg1* was confirmed during RT-qPCR and western blot experiments as well. (B) In vitro luciferase experiment demonstrated decreased *Pttg1* promoter activity after ASA and decitabine treatment. Although in human pituitary adenomas global demethylation level did not show significant association with *PTTG1* expression (C), upon ASA administration significant negative correlation was observed between *Pttg1* expression and 5hmC level (B).

Figure 6. ASA -demethylation-*Pttg1*-*Tp53* regulatory network. In pituitary adenoma ASA increased global demethylation by elevating *TET1-3* enzyme level. Global DNA methylation induces global transcriptional alteration including *Pttg1* underexpression that was validated by decitabine treatment. Additionally, ASA inhibits *Pttg1* promoter activity. Independently, ASA acetylated p53 leading to increased p53 stability and enhanced transcriptional activity (Reed et al. 2014). *Pttg1* inhibits p53 activity as it reduces p53 protein stability and represses its transcriptional activity (Read et al.2018). As a summary, upon ASA treatment global transcription alteration, and enhanced p53 activity results in inhibition of cell cycle, proliferation, viability. See details in the discussion.

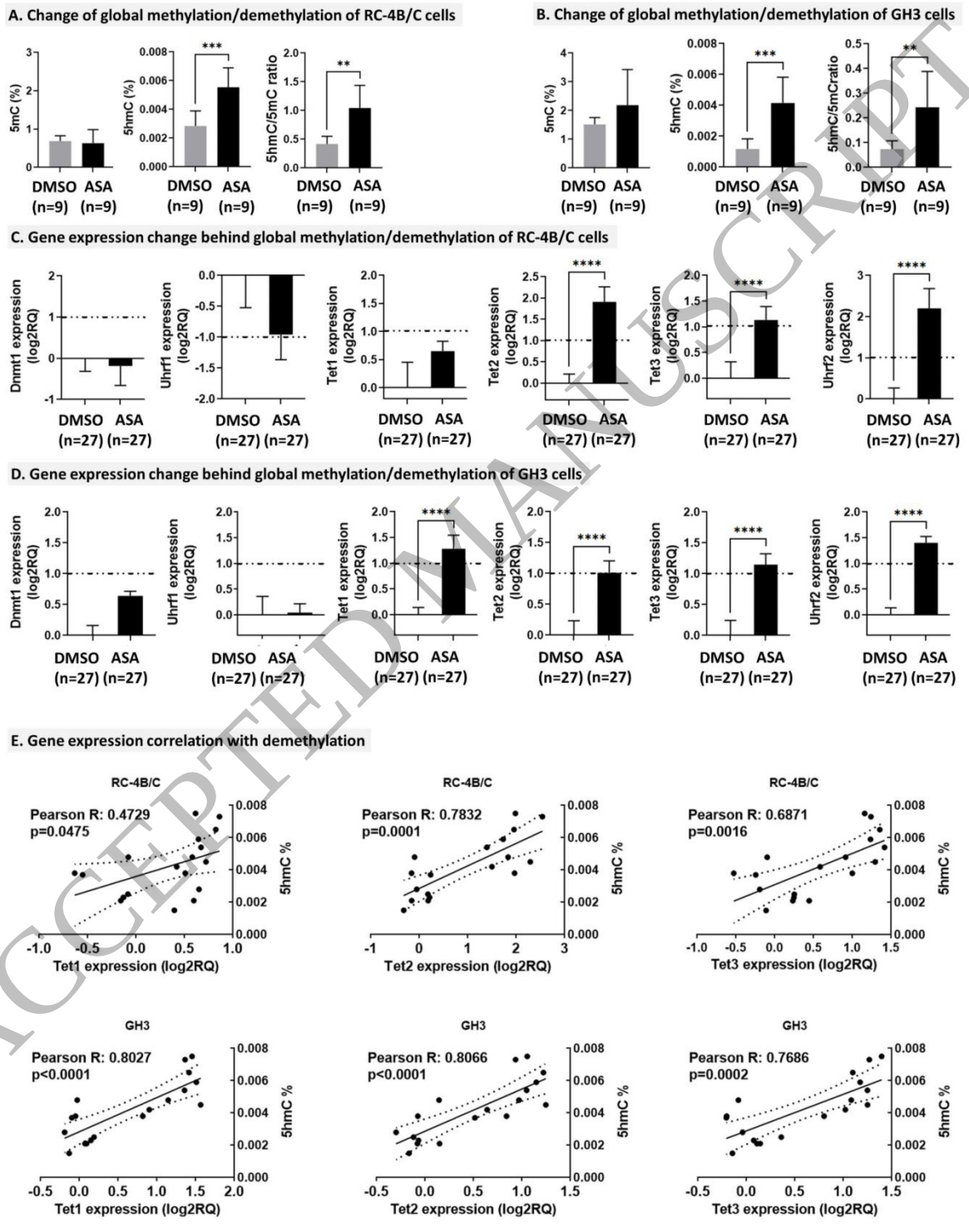

Figure 1
160x226 mm (x DPI)

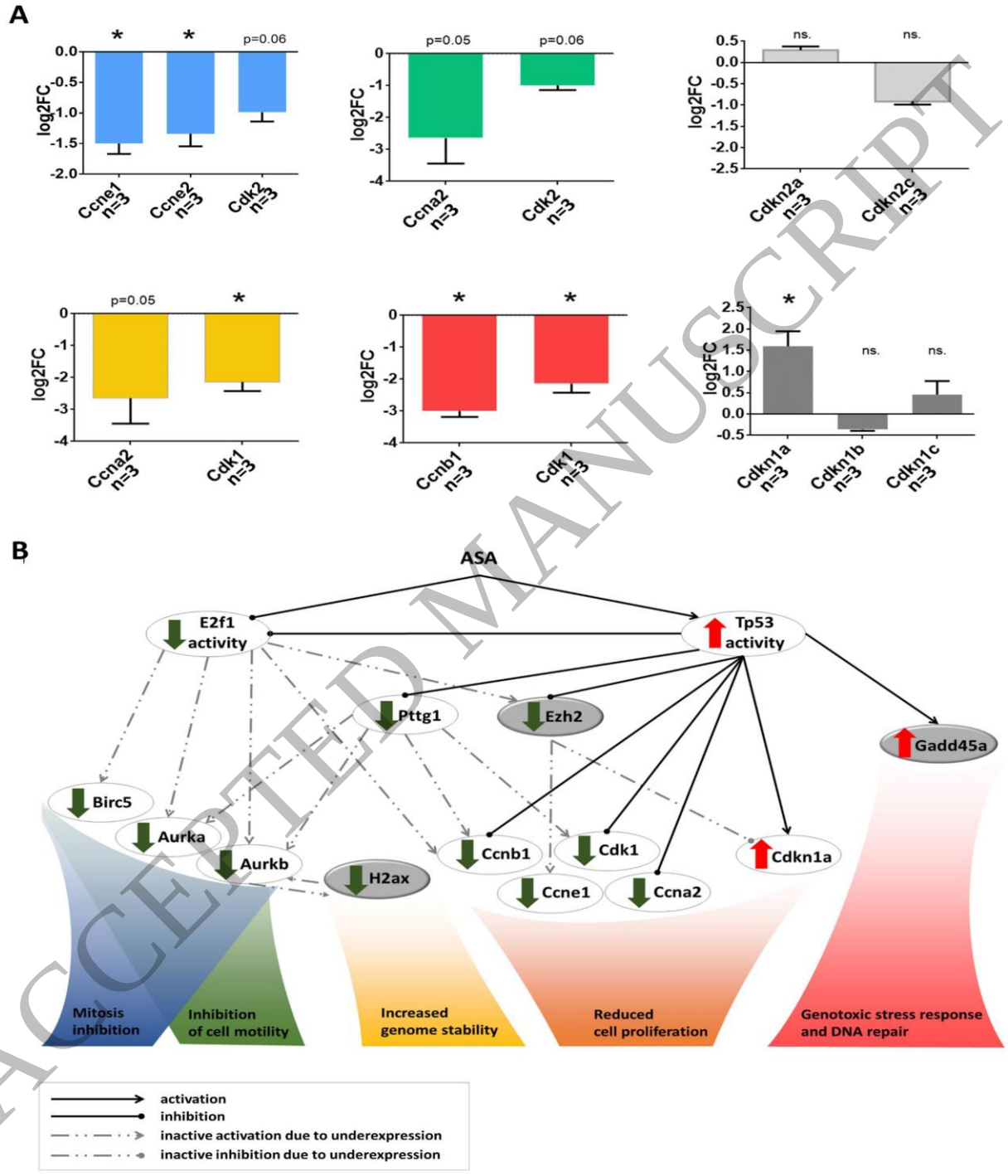

Figure 2
160x238 mm (x DPI)

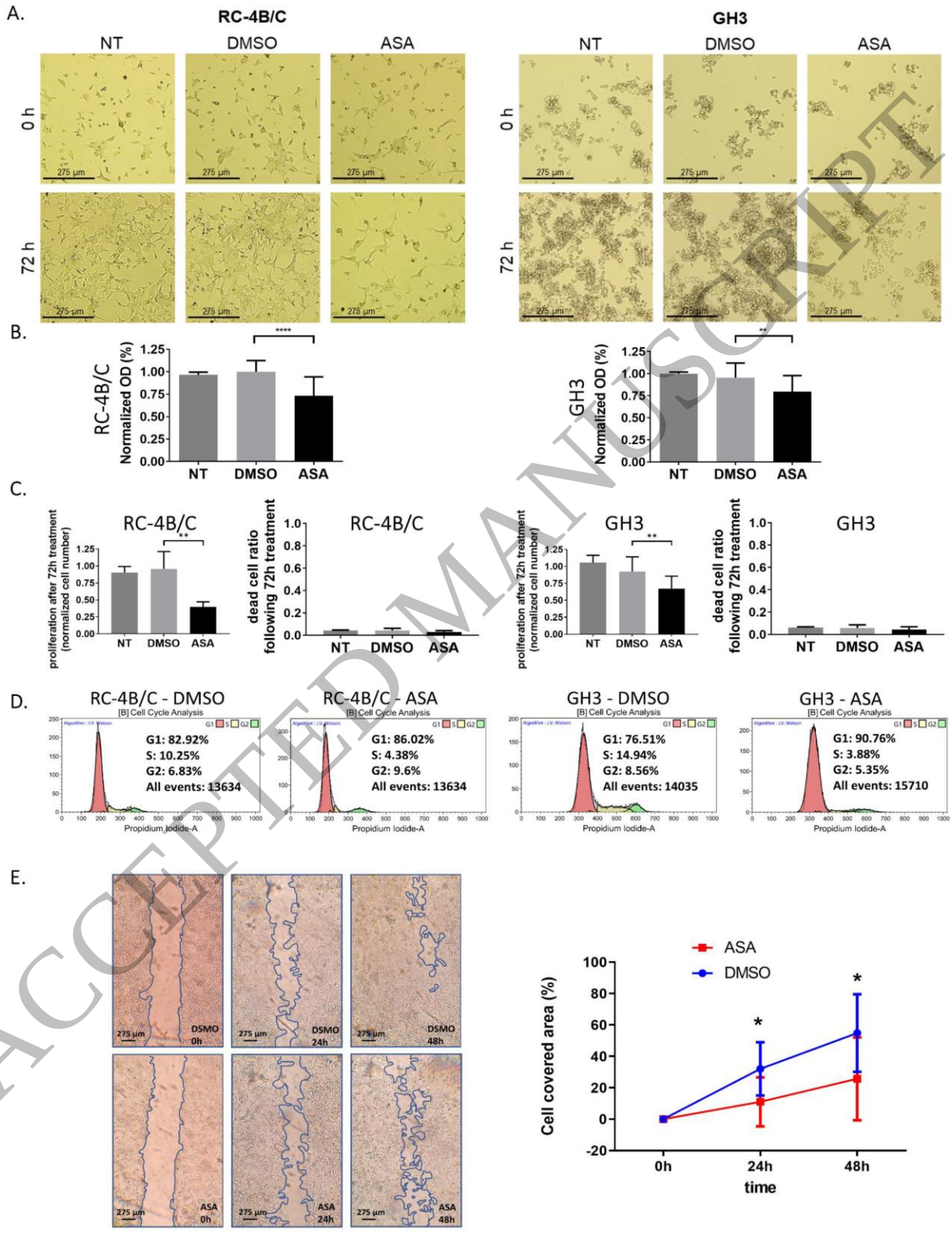

Figure 3
160x224 mm (x DPI)

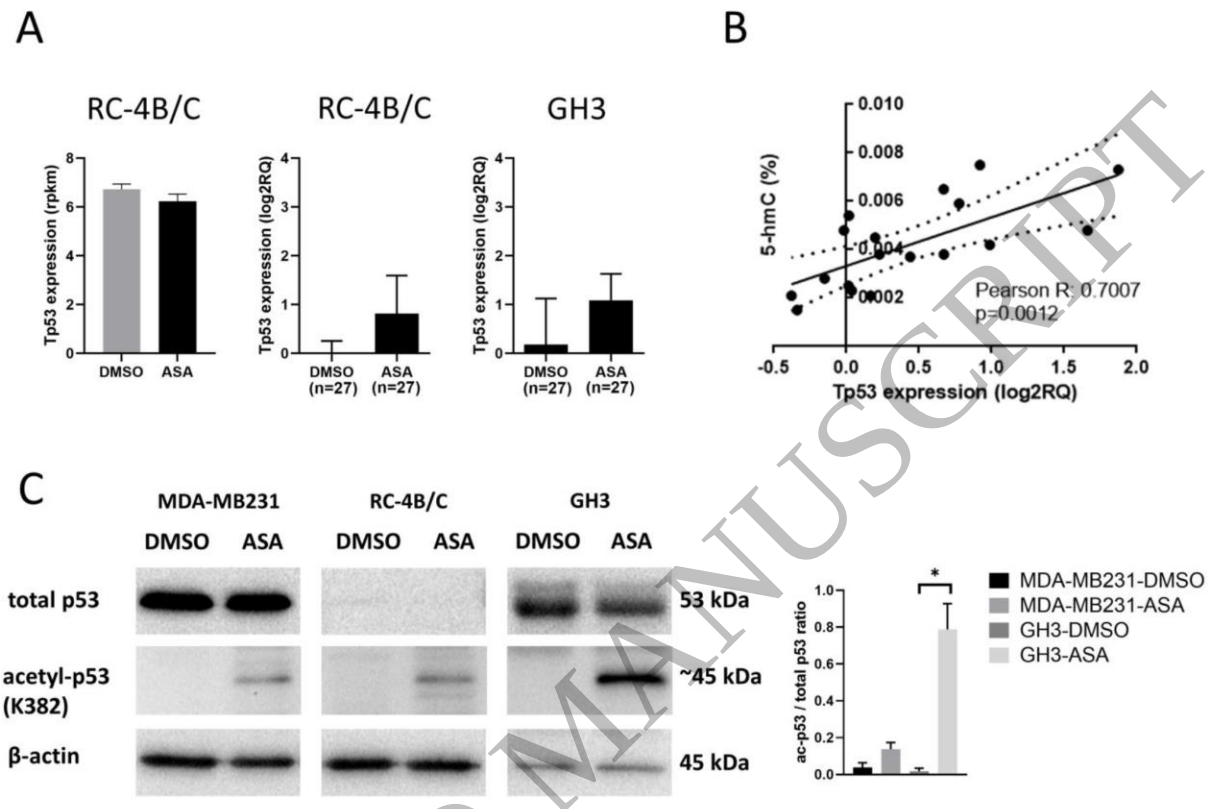

Figure 4
160x110 mm (x DPI)

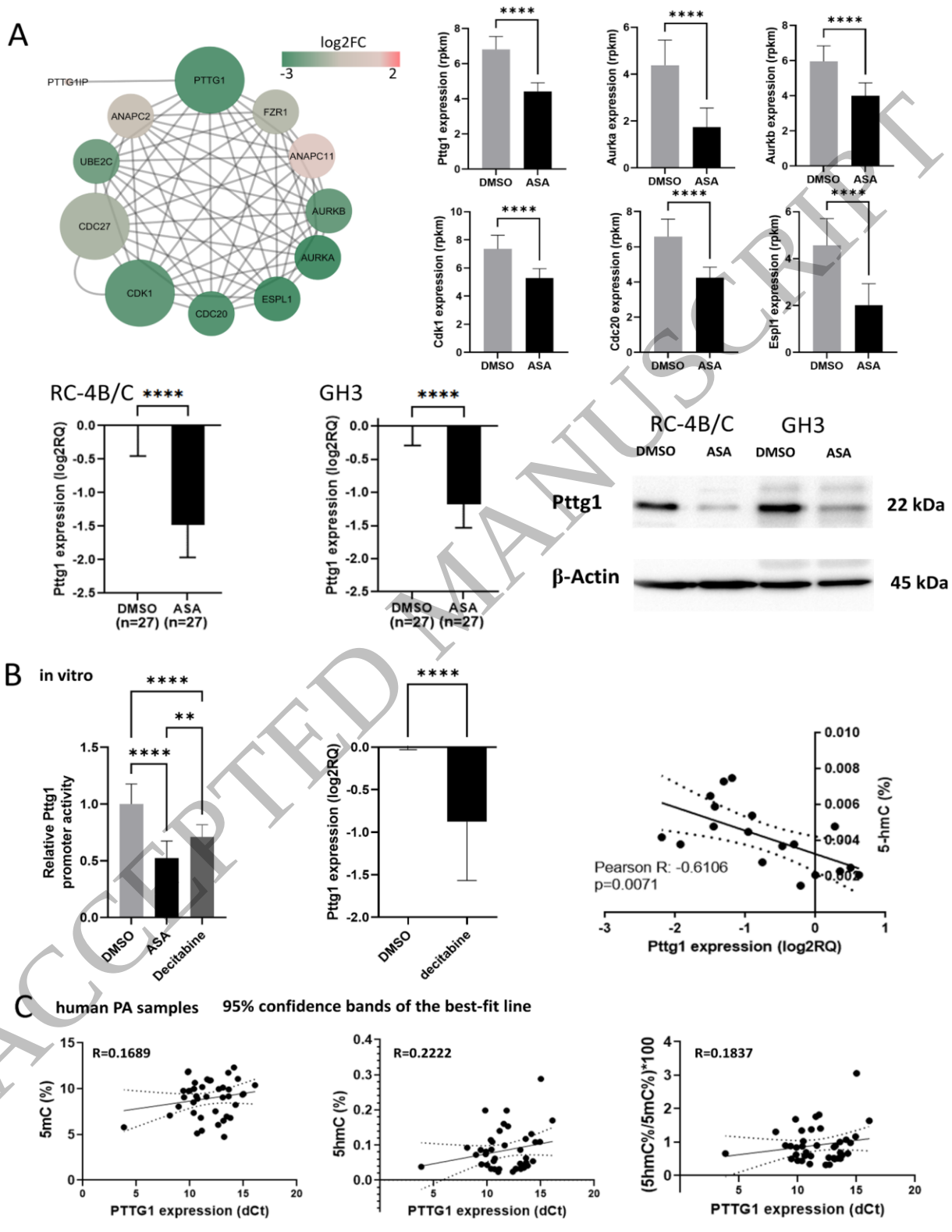

Figure 5
160x225 mm (x DPI)

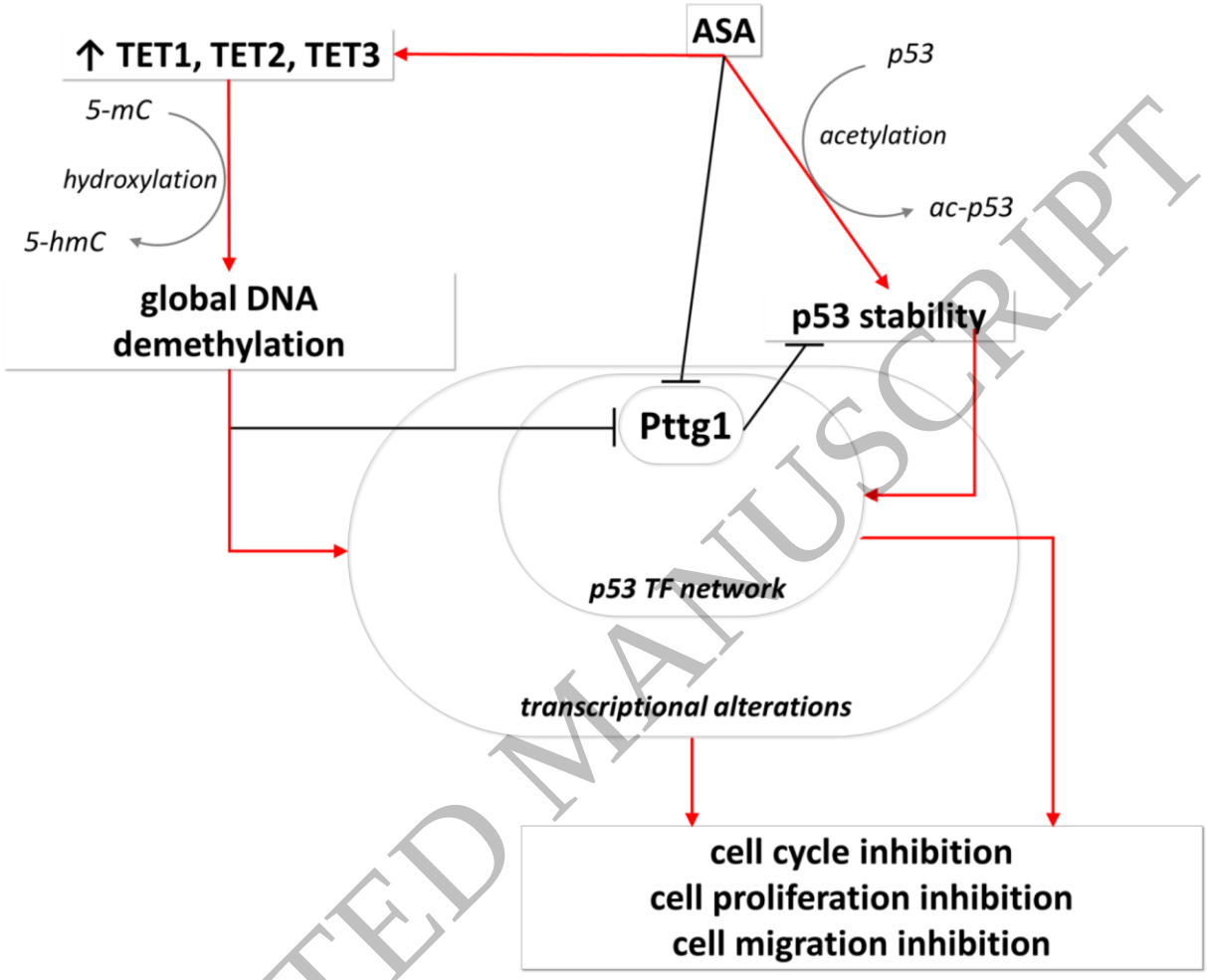

Figure 6
160x133 mm (x DPI)